Open Channel Block by Ca^{2+} Underlies the Voltage Dependence of *Drosophila* TRPL Channel

Moshe Parnas, Ben Katz, and Baruch Minke

Department of Physiology and the Kühne Minerva Center for Studies of Visual Transduction, Faculty of Medicine, Hebrew University, Jerusalem 91120, Israel

The light-activated channels of *Drosophila* photoreceptors transient receptor potential (TRP) and TRP-like (TRPL) show voltage-dependent conductance during illumination. Recent studies implied that mammalian members of the TRP family, which belong to the TRPV and TRPM subfamilies, are intrinsically voltage-gated channels. However, it is unclear whether the *Drosophila* TRPs, which belong to the TRPC subfamily, share the same voltage-dependent gating mechanism. Exploring the voltage dependence of *Drosophila* TRPL expressed in S2 cells, we found that the voltage dependence of this channel is not an intrinsic property since it became linear upon removal of divalent cations. We further found that Ca^{2+} blocked TRPL in a voltage-dependent manner by an open channel block mechanism, which determines the frequency of channel openings and constitutes the sole parameter that underlies its voltage dependence. Whole cell recordings from a *Drosophila* mutant expressing only TRPL indicated that Ca^{2+} block also accounts for the voltage dependence of the native TRPL channels. The open channel block by Ca^{2+} that we characterized is a useful mechanism to improve the signal to noise ratio of the response to intense light when virtually all the large conductance TRPL channels are blocked and only the low conductance TRP channels with lower Ca^{2+} affinity are active.

The Journal of General Physiology

INTRODUCTION

TRP cation channels play an important role in signal transduction of numerous organisms. For example, in *Drosophila,* TRP channels are known to mediate the response to light (Ranganathan et al., 1995; Scott and Zuker, 1998; Montell, 1999; Hardie and Raghu, 2001; Minke and Cook, 2002) and in mammals they are involved in detections of changes in the environment. TRP channels gate in response to a myriad of stimuli, including cold or hot temperatures, natural chemical compounds (menthol, camphor, and capsaicin), and mechanical stimuli. These channels are crucially involved in physiological processes, e.g., photoreception, pheromone sensing, taste perception, thermosensation, pain perception, mechanosensation, perception of pungent compounds (mustard, garlic), renal Ca^{2+}/Mg^{2+} handling, smooth muscle tone, and blood pressure regulation (Minke and Cook, 2002; Clapham, 2003; Voets et al., 2004, 2005; Montell, 2005; Nilius et al., 2005; Pedersen et al., 2005; Nilius and Mahieu, 2006). There are seven TRP subfamilies: TRPC, which includes the founding member of this family, the *Drosophila* TRP (Minke et al., 1975), TRPM, TRPV, TRPN, TRPA, TRPP, and TRPML (Clapham et al., 2005; Montell, 2005; Owsianik et al., 2005). In spite of the vast interest in these channels, the mechanism underlying stimulus-dependent regulation and gating of TRP channels remains largely unknown (Clapham et al., 2005).

Recent studies conducted in heterologous expression systems implied that members of the TRPV and TRPM subfamilies are voltage-gated channels, showing a temperature- and agonist-dependent shift of their voltage dependence (Voets et al., 2004; Clapham et al., 2005). It is, however, unclear whether other subfamilies of TRP channels share the same voltage-dependent gating mechanism (Nilius et al., 2005).

The *Drosophila* photoreceptor cell is a powerful experimental system, currently being one of the few systems in which two members of the TRPC family, TRP and TRPL, are accessible to whole cell recordings and their physiological functions are well defined in vivo (Ranganathan et al., 1995; Scott and Zuker, 1998; Montell, 1999; Hardie and Raghu, 2001; Minke and Cook, 2002). However, the photoreceptor cells are not accessible to single channel recordings of the native TRP and TRPL channels (Hardie, 1991; Ranganathan et al., 1991). Often, channels expressed in heterologous systems differ in their properties from in vivo channels (Minke and Parnas, 2006). This, however, is not the case for the expressed TRPL channels in *Drosophila* S2 cells, as they show similar properties to the native channel (Hardie et al., 1997). Therefore, results obtained in S2 cells expressing TRPL channels, which allows single

M. Parnas and B. Katz contributed equally to this work.
Correspondence to Baruch Minke: minke@md.huji.ac.il

Abbreviations used in this paper: CaM, calmodulin; CNG, cyclic nucleotide-gated; LIC, light induced current; S2, Schneider 2 cells; TRP, transient receptor potential; TRPL, TRP-like.

TABLE I

Extracellular Solutions

Number	Name	NaCl		KCl	$MgSO_4$ (P^a) / $MgCl_2$ (S2)	TES	Proline	Alanine	$CaCl_2$	EGTA	EDTA
		P^a	S2								
1	1.5 mM $CaCl_2$	120	130	5	4	10	25	5	1.5	–	–
2	Low divalents	120	130	5	4	10	25	5	–	1	–
3	Divalent free	125	130	5	–	10	25	5	–	–	1/5

[a]Photoreceptor.

channel analysis (see below), can be verified and provide physiological insight to the native system.

In the present study we explored the voltage dependence of expressed *Drosophila* TRPL channels and show that it is not an intrinsic property of the channels, but arises from voltage-dependent Ca^{2+} open channel block. A mathematical model constructed from experimental observations describing channel–Ca^{2+} interaction indicated that it is the dissociation of Ca^{2+} from the open channel that underlies the voltage dependence of the channel. Whole cell recordings from a *Drosophila* mutant expressing the native TRPL channels indicated that Ca^{2+} block also accounts for the voltage dependence of the native TRPL channels in the photoreceptor cells.

MATERIALS AND METHODS

Fly Stocks

White-eyed trp^{P343} null mutants were used.

Light Stimulation

A xenon high-pressure lamp (PTI, LPS 220, operating at 50 W) was used, and the light stimuli were delivered to the ommatidia by means of epi-illumination via an objective lens (in situ). The intensity of the orange light (Schott OG 590 edge filter) at the specimen, with no intervening neutral density filters, was 13 mW/cm^2.

Cell Culture

Schneider S2 cells were grown in 25-cm^2 flasks at 25°C in Schneider medium (Beit Haemek Biological Industries) supplemented with 10% FBS and 1% pen-strep. In the present study we used stably expressed TRPL-eGFP channels. Table S1 (available at http://www.jgp.org/cgi/content/full/jgp.200609659/DC1) show that there is no significant difference in the major properties of the TRPL- and TRPL-eGFP–expressed channels used in the current study.

Electrophysiology

For S2 cells, cells were seeded on polylysine-coated plates at a confluence of 25%, 24–72 h before the experiment. 24 h before the experiment, 500 μM $CuSO_4$ was added to the medium to induce expression of the TRPL-eGFP channel. For *Drosophila* ommatidia, dissociated *Drosophila* ommatidia were prepared from newly emerged flies (<1 h after eclosion) and whole-cell, patch-clamp recordings were performed as previously described (Peretz et al., 1994). Whole-cell and single-channel currents are recorded at room temperature using borosilicate patch pipettes of 5–8 MΩ and an Axopatch 1D (Axon Instruments, Inc.) voltage-clamp amplifier. For single channel recordings, pipettes were coated with Dow Corning sylgard. For S2 cells, voltage-clamp pulses were generated and data were captured using a Digidata 1322A interfaced to a computer running the pClamp 9.2 software (Axon Instruments, Inc.). For *Drosophila* ommatidia, Digidata 1200 and pClamp 8.0 software (Axon Instruments, Inc.) were used. Currents were filtered using the 8-pole low pass Bessel filter of the patch-clamp amplifier at 10 kHz and sampled at 50 kHz (single channel recordings) or filtered at 5 kHz and sampled at 20 kHz (whole cell recordings). To measure I-V curves with minimal distortions, only cells with low (<10 MΩ) series resistance were used and the series resistance was compensated to ~80%.

Solutions

The details of the solutions are presented in Tables I and II. All solutions were titrated to pH 7.15. Free Ca^{2+} was estimated using MaxChelator v. 2.50 (http://maxchelator.stanford.edu/) using tables cmc0204e.tmc and the following parameter settings: t = 25°C, pH = 7.15, I = 163.

Data Analyses and Model Simulations

Data is analyzed and plotted using pClamp 9.2 software (Axon Instruments, Inc.) and Sigma Plot 8.02 software (Systat Software, Inc.). For kinetics analyses, the probability of single channel openings (if there are actually two channels present) was estimated according to the equation given by Colquhoun and Sigworth (1995).

$$P(r \geq n_o) = \pi^{n_o - 1}$$

$$\pi = \frac{1 - P_o}{1 - \frac{P_o}{2}},$$

where n_o is the number of single openings. Single-channel events were identified on the basis of the half-amplitude threshold-crossing criteria. Histograms of open and closed durations were constructed conventionally as distributions of the logarithm of duration (in ms, 15 bins per decade) with exponential components fitted by the method of maximum likelihood (Colquhoun and Hawkes, 1995). The frequency density and fitted functions were plotted after a square root transformation. The number of probability density function components was determined using the automatic "compare models" routine of the pClamp 9.2 software at the confidence level of 0.99. Current amplitude histograms are fitted with Gaussian functions. Burst analysis was performed using the pClamp 9.2 automatic search with the maximum interval method of 1- and 5-ms intervals between bursts. For event histograms, only events longer than twice T_r were used (Colquhoun and Hawkes, 1995). The event histogram, which was constructed by this method, does not represent the channel open probability but the number of events.

Model Simulation

We used a stochastic model (Gillespie, 1977) to simulate single channel activity and a differential model to simulate whole cell activity. Both models were solved using MATLAB 6.5 software.

TABLE II

Intracellular Solutions

Number	Name	CsCl	TES	TEA	K_2ATP	NaGTP	β-NAD	EGTA	EDTA
4	1.5 mM $CaCl_2$	125	10	15	–	–	–	–	–
5	Low divalents	125	10	15	–	–	–	1	–
6	Divalent free	125	10	15	–	–	–	–	5
7	1.5 mM $CaCl_2$	120	10	15	4	0.4	1	–	–
8	Low divalents	120	10	15	4	0.4	1	1	–
9	Divalent free	120	10	15	4	0.4	1	–	5

Online Supplemental Material

The supplemental material (available at http://www.jgp.org/cgi/content/full/jgp.200609659/DC1) includes two sections. The first section explains how the rate constants of the model were derived experimentally. The second section contains three model insights: (1) an explanation of why the short blocked state cannot be observed experimentally; (2) demonstration of burst stabilization at positive membrane potential by the blocked state; and (3) detailed explanation of why the dissociation of divalent ions from the blocked state is voltage dependent. In addition, the supplemental material includes three tables and a figure (Tables S1–S3 and Fig. S1): (1) a comparison between expressed TRPL and TRPL-GFP; (2) actual data used to derive the above rate constants; (3) the parameters of the voltage-dependent divalent block model; and (4) a figure demonstrating the above three model insights.

RESULTS

The Outward Rectification of Heterologously Expressed TRPL Channels Is Not an Intrinsic Property but Depends on the Presence of Divalent Cations

To explore, for the first time, the voltage dependence of *Drosophila* light-activated conductance at the single channel level, we used TRPL channels expressed in *Drosophila* S2 cells. This is because the native *Drosophila* TRP and TRPL channels are not accessible to single channel recordings (Hardie, 1991; Ranganathan et al., 1991) and heterologous expression of functional TRP channels has proven unsuccessful (Minke and Parnas, 2006).

Cell-attached patch clamp recordings from S2 cells expressing TRPL, at various membrane voltages in the presence of divalent ions, revealed a large increase in channel activity with the increase in membrane potential (Fig. 1 A). Consistent with the cell-attached data, whole cell recordings showed that cells expressing TRPL displayed outwardly rectifying I-V curves (using voltage ramps from −150 to 150 mV in 1 s) when exposed to extracellular solutions containing either Ca^{2+} or Ba^{2+} ions (Fig. 1 B, green and black curves, respectively). Removal of divalent cations from the extracellular solution resulted in an increase of inward current but did not cause a full linearization of the I-V curve (pink curve). When both intracellular and extracellular solutions were divalent free, the channels exhibited a linearization of the I-V curve (blue curve, $n = 11$). The outward rectification of the I-V curve could be restored upon application of external Ca^{2+} or Ba^{2+} (Fig. 1 B, green and black curves, respectively). It can be argued that in the absence of divalent cations, the membrane becomes fragile and gives rise to a large leak current, which underlies the linear I-V curve. This possibility was ruled out by the following observations. First, Fig. 1 B shows that the divalent free solution affected only the currents at the negative membrane potentials (from −200 pA to approximately −2,000 pA), while at positive membrane potentials the currents remained virtually the same. Second, the reversal potential during divalent-free solution was ∼15 mV and not zero as expected from leak current, consistent with the reversal potential of intracellular Cs^+ solution and extracellular Na^+ solution. Third, after establishing a linear I-V curve, we applied either Ca^{2+}- or Ba^{2+}-containing solutions, and the outward rectification was reestablished (Fig. 1 B).

To further quantitate the blocking effect of Ca^{2+}, we measured the affinity of Ca^{2+} to the TRPL channel (Fig. 1 C). The affinity was calculated by measuring the degree of Ca^{2+} block on the inward current during whole cell recordings using Ca^{2+}-EGTA and Ca^{2+}-EDTA buffer solutions, and a Kd of 163 ± 5 nM was measured (Fig. 1 C). The high affinity of TRPL to Ca^{2+} and the steep dependence of the Ca^{2+} block on TRPL channel activity have important physiological implications (see Discussion).

The results of Fig. 1 (A–C) indicate that the voltage dependence of the expressed TRPL channel is not an intrinsic property but arises from a high-affinity Ca^{2+} block, which is relieved at positive membrane voltage.

Voltage-dependent Change in the Opening Frequency of the TRPL Channel Underlies the Outward Rectification Observed in the Presence of Divalent Cations

To unravel the mechanism underlying the voltage-dependent I-V relationship of expressed TRPL channels and its dependence on Ca^{2+}, we employed single channel measurements. Excised inside-out patches with pipettes containing divalent-free solution revealed that patches exposed to divalent-containing solution at the intracellular side showed no channel activity at the negative membrane potential and a significant activity at the positive membrane potential (Fig. 1 D, left). Membrane patches exposed to divalent-free solution

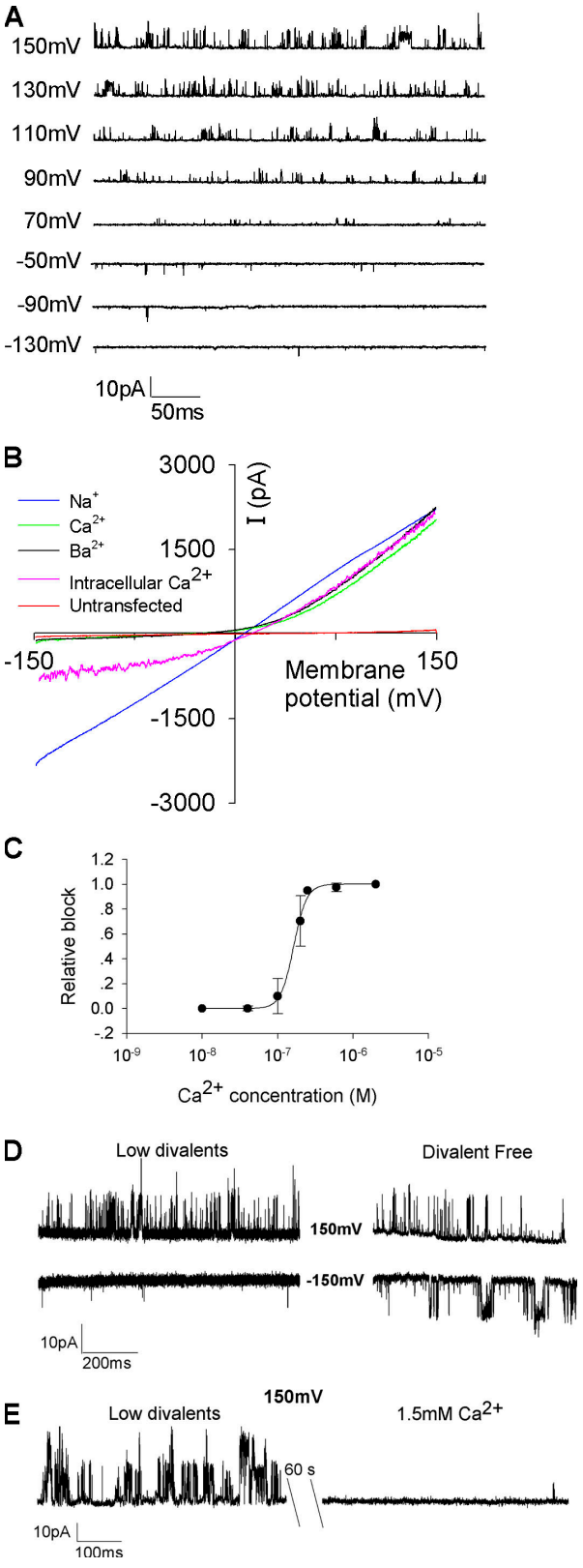

Figure 1. Divalent block underlies the outward rectification of the TRPL channel. (A) Cell-attached recordings from S2 cells at various membrane voltages as indicated in the presence of divalent ions (solutions 2 and 5 in Tables I and II). (B) Family of I-V curves measured by whole-cell patch clamp recordings using voltage ramp from −150 to 150 mV in 1 s (voltage ramps from 150 to −150 mV showed the same behavior). Before expression of TRPL, the cells show only a small leak current (red curve). The cells were initially bathed in 130 mM NMDGCl solution; the bath solution was then replaced by 130 mM NaCl + 1 mM EGTA solution ($n = 11$). Then, the cells were perfused with 130 mM NaCl + 1.5 mM Ca^{2+} or 1.5 mM Ba^{2+}. (C) The affinity of Ca^{2+} to the TRPL channel. The relative blocking effect of Ca^{2+} on the inward current of the I-V curve is plotted as a function of Ca^{2+} concentration, which was obtained by various concentrations of Ca^{2+} solutions. A linear I-V curve was initially obtained using a solution containing 40 nM free Ca^{2+}. Then, a series of solutions with increased Ca^{2+} concentrations were perfused, until total block was obtained. The relative block was calculated by dividing the currents at different Ca^{2+} concentration with the current obtained at the lowest Ca^{2+} concentration. The calculated affinity of the TRPL channel to Ca^{2+} was 163 ± 5 nM (error bars indicate SEM in all relevant figures, $n = 3$–5). (D, left) Excised inside out patch clamp recordings, initially perfused at 130 mM NaCl + 1 mM EGTA + 4 mM Mg^{2+} at 150 and −150 mV membrane potentials. (D, right) The paradigm of the left panel was repeated except that the divalent-free solution was used with 130 mM NaCl + 1 mM EDTA. (E) Excised inside out patch clamp recordings; the bath solution containing low divalent (see D, left) was changed to solution containing 1.5 mM Ca^{2+} ($n = 7$).

showed similar channel activity at both negative and positive membrane potentials (Fig. 1 D, right). Ca^{2+} exerted a more profound inhibition from the intracellular side relative to the extracellular side. This conclusion was derived from the complete inhibition of channel activity even at positive membrane potentials in excised inside out patches when exposed to 1.5 mM Ca^{2+} (Fig. 1 E), while significant current was still observed in whole cell recordings in the presence of the same Ca^{2+} concentration in the extracellular solution.

Several mechanisms could account for the Ca^{2+}-dependent outward rectification of the TRPL channel. To determine if divalent cations could affect single channel conductance in a voltage-dependent manner, we examined the effect of membrane potential on various channel parameters in the presence of divalent cations. To measure the single channel conductance, we applied voltage ramps (from −150 to 150 mV in 1 s) in an excised inside out membrane patch that contained only few channels. The low frequency of channel activity at negative membrane potentials (Fig. 1 A) made it difficult to obtain an I-V curve of single channel open conductance at negative membrane potentials. To overcome this difficulty we used superimposed current traces during voltage ramps from the same cell. In some cells after application of many voltag ramps, the frequency of channel openings increased spontaneously, showing many channel openings at negative membrane potentials, while at positive membrane potentials, the channel was virtually constantly open and relatively small closing events were observed. Fig. 2 A presents an example of such recording. The straight line is a linear

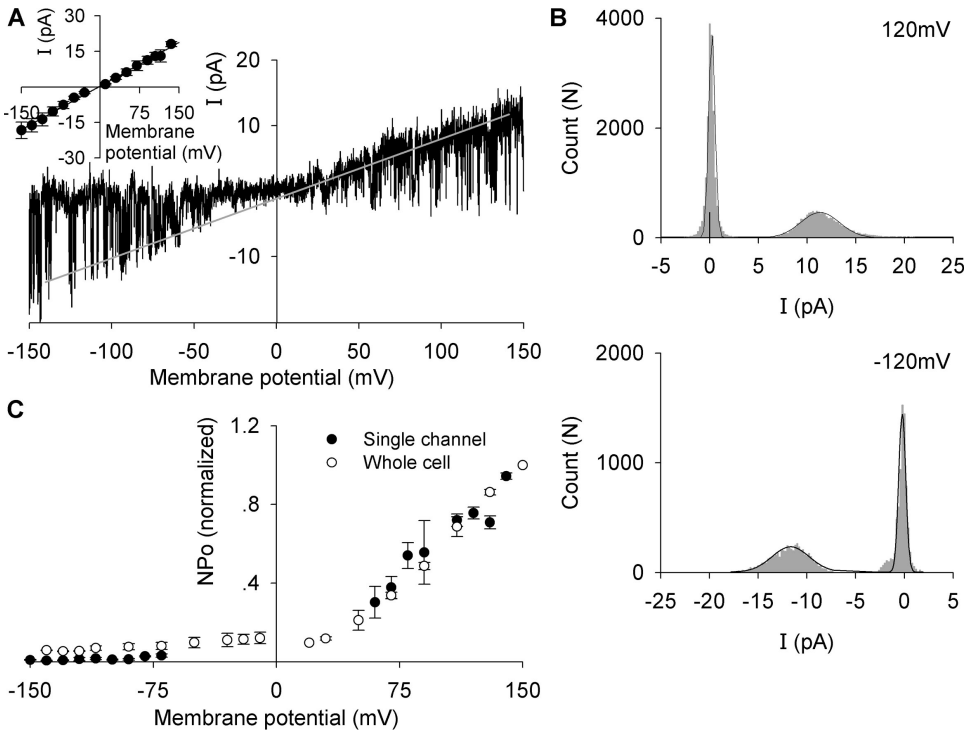

Figure 2. Voltage dependence of the open probability of the TRPL channel underlies its outward rectification (the solutions used in this figure are 2 and 5 in Tables I and II). (A) Single channel recordings from excised inside out patch during voltage ramp from −150 to 150 mV in 1 s. In the cell presented in A, the open probability of the channel was very high, with virtually no closures at positive membrane potentials, and a relatively high opening frequency at negative membrane potentials. This cell yielded the same single channel conductance as other cells and made it possible to observe channel openings at negative membrane potentials. The straight line is a linear regression through channel openings of long duration. Inset, single channel I-V curve obtained from voltage steps; channel conductance of 110 pS was calculated (error bars represent SEM, $n = 5$). (B) Event histograms (see Materials and methods) at two membrane potentials, 120 (top) and −120 mV (bottom) in the presence of divalent ions. A single Gaussian fits the open state. Note the different scales. (C) Normalized voltage dependence of the TRPL channel open probability. ●, plots of the open probability obtained from single channel recordings in cell attached mode with low divalent solution. ○, plots of the open probability obtained from whole cell recordings with low divalent extracellular solution ($n = 3$).

regression curve fitting only the long channel openings. This curve also fits superimposed current traces of voltage ramps from the same cell before the enhanced channel activity was developed. A linear I-V curve of the open state of the channel was observed (Fig. 2 A, gray line). A single channel conductance of 110 pS ($n = 5$) was measured (Fig. 2 A inset), which is similar to that obtained in a previous systematic study (Zimmer et al., 2000), but differs from earlier reports by about a factor of 2 (Hardie et al., 1997). This discrepancy most likely arose from the different method used to calculate single channel conductance in the latter study. Hardie et al. (1997) mainly used noise analysis from whole cell recordings, which usually gives a rough estimate of the actual single channel conductance. Indeed, several studies in which the single channel conductance of the expressed TRPL channel was determined directly from single channel analysis revealed single channel conductance very similar to that obtained in the present study, although different expression cell systems were used (i.e., COS, HEK, and Sf9 cells; Obukhov et al., 1996; Kunze et al., 1997; Hambrecht et al., 2000).

Fig. 2 A thus demonstrates that the open channel behaves as an ohmic resistor, ruling out the possibility of changes in single channel conductance as the source of the voltage dependence.

To further examine whether the outward rectification is due to the existence of several levels of channel conductance, we constructed event histograms (see Materials and methods) for the entire range of membrane potentials. Fig. 2 B shows two examples from positive (top) and negative (bottom) membrane potentials. A single Gaussian produced a best fit for the current distribution, indicating that the TRPL channel has only one channel conductance.

To address the possibility that the dependence of channel open probability, P_o, on membrane potential underlies the voltage dependence of the channel, we measured P_o directly as a function of membrane potential. Fig. 2 C shows that P_o depends on membrane potential. This conclusion is reached irrespective of the method used to calculate P_o (single channel patch clamp or whole cell recordings; Fig. 2 C, filled circles and open circles, respectively). The voltage dependency of P_o could result from the effect of voltage on the number of channel openings (opening frequency) or from the effect on the mean open time. The results of Fig. 3 A revealed that voltage affected the opening frequency. In particular, the channel opening frequency increases as depolarization increases (the number of channel openings at −150 mV is only 5% of that at 150 mV). The observed frequency of channel openings measured from single channel recordings correlates well with the

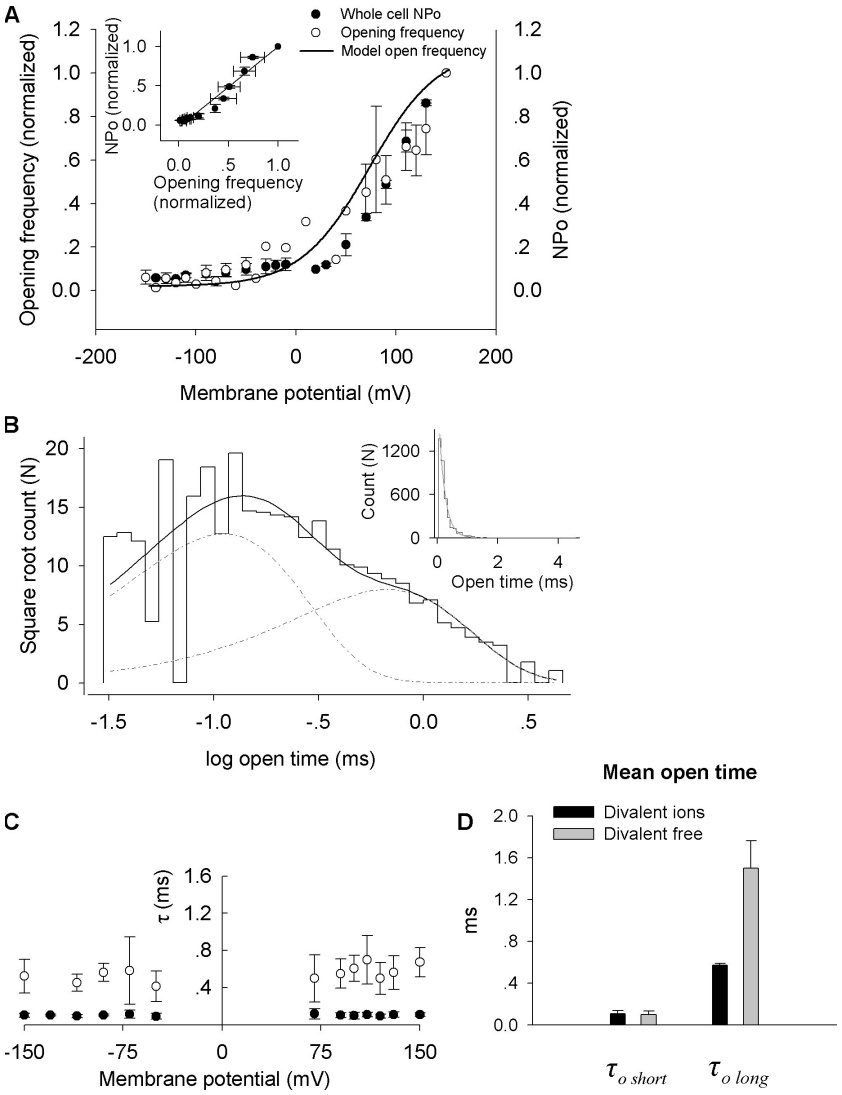

Figure 3. The voltage and Ca^{2+}dependence of the TRPL channel. (A) ○, normalized voltage dependence of the number of channel openings obtained from single channel recordings (error bars: SEM, n = 2–11). ●, open probability obtained from whole cell recordings (same as Fig. 2 C). The solid line is a model calculation of divalent block. Inset, the open probability is plotted against the opening frequency (adjusted R^2 = 0.98). (B) An open time histogram of the TRPL channel openings. Two time constants were observed: a fast one of 0.1 ± 0.01 ms (n = 9) and a slower one of 0.57 ± 0.02 ms (n = 13). Inset, the data is presented on a linear scale. (C) A plot of the open states time constants (mean open time) as a function of membrane voltage (n = 3–13). ● and ○ represent the short and long closing time constant, respectively. (D) Histogram plotting the mean open time of the short and long open states. The figure shows that the time constant of the long open state is affected by divalent ions (n = 4) (solutions 2, 5 and 3, 6 in Tables I and II).

channel open probability measured from whole cell recordings (Fig. 3 A, inset) and the two different measurements fit a curve (Fig. 3 A, solid line) derived from model calculations of divalent block (for details on the model see below and Fig. 4 A). This close fit suggested that voltage dependence of the opening frequency is sufficient to account for the voltage dependence of the open probability.

We next examined whether the mean open time is also voltage dependent. An open time histogram is presented in two ways: in linear (Fig. 3 B, inset) and log scales (Fig. 3 B). The histogram in log scale is more revealing (Colquhoun and Hawkes, 1995) and could be fitted by two exponents of a short time constant (0.1 ± 0.01 ms) and a longer time constant (0.57 ± 0.02 ms; n = 11). The calculated values of the mean open time are plotted in Fig. 3 C as a function of membrane potential. In contrast to the frequency of channel openings (Fig. 3 A), the two time constants of channel closing, which determine the mean open time, show no voltage dependence. Thus, the frequency of channel openings is the sole parameter that determines the voltage dependence of the TRPL channel.

Ca^{2+} Inhibits the TRPL Channels via an Open Channel Block Mechanism

The data presented in Fig. 1 revealed a strong inhibitory effect of Ca^{2+} on TRPL channel openings. Therefore, we further examined the mechanism underlying this Ca^{2+}-dependent inhibition and its relationship to the apparent voltage dependence of the channel (Figs. 2 and 3). The observation that two exponents are required to best fit the open time histogram (Fig. 3 B) suggests that two open states of long and short open time exist, though only a single conductance characterizes both (Fig. 2 B). The mean open time of both open states is voltage independent (Fig. 3 C). Given the strong inhibition of Ca^{2+} on channel openings, (Fig. 1) we investigated whether the mean open time is Ca^{2+} dependent. Importantly, the open time histogram (Fig. 3 D) exhibited

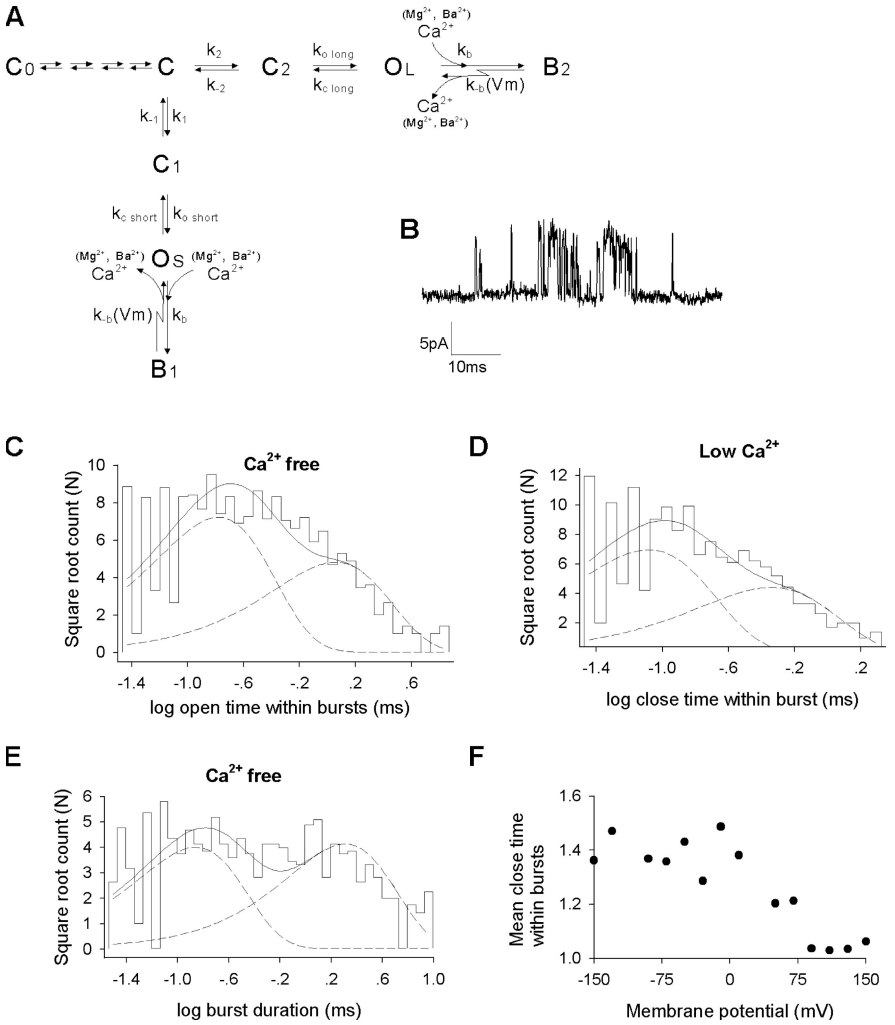

Figure 4. Kinetic model that accounts for the voltage-dependent divalent block of the TRPL channel. (A) Kinetic model. C, O, and B are closed, open, and blocked states respectively. Note that the voltage dependence according to the model is at the dissociation of Ca^{2+} from the blocked states. (For details see online supplemental material.) (B) Typical bursting behavior obtained during single channel recordings in cell-attached mode at 150 mV membrane potential. (C) Open time histogram from channel openings obtained only from bursts. Two time constants are shown, a fast time constant of 0.18 ± 0.01 ms and a slow time constant of 0.85 ± 0.07 ms (n = 8–17) (solutions 3 and 6 in Tables I and II). (D) Closed time histogram obtained only from bursts in low divalent cation–containing solution. Two time constants are shown, a fast one of 0.17 ± 0.01 ms and a slower one of 0.58 ± 0.13 ms (n = 12) (solution 2 in Table I). (E) Burst duration histogram obtained from cells at divalent free solution. Two time constants are shown, a fast one of 0.11 ± 0.03 ms and a slower one of 1.6 ± 0.26 ms (n = 4) (solutions 3 and 6 in Tables I and II). (F) The mean closed time within the burst is plotted as a function of the membrane potential (n = 4).

two time constants, where the fast one was not sensitive to divalent cations (Fig. 3 D, left), while the slow one was ~2.5-fold faster in the presence of divalent cations (Fig. 3 D, right). The results of Fig. 3 D further indicate that only the long open state is susceptible to open channel block, presumably because the short open state is too short to allow a Ca^{2+} block (see model insights in the online supplemental material, available at http://www.jgp.org/cgi/content/full/jgp.200609659/DC1). Together, the data of Figs. 1–3 indicate that Ca^{2+} blocks the open channel because it affects the duration of channel openings (open channel block). In addition, depolarization relieves the channel from the Ca^{2+} block, a typical characteristic of open channel block mechanism.

A Kinetic Model that Accounts for the Open Channel Block by Divalent Cations

To better understand and characterize the properties of the TRPL channel in general and the nature of the Ca^{2+} block in particular, we constructed a minimal kinetic model of the channel states (Fig. 4 A). In constructing the model we were guided by the previously shown experimental results. Specifically, Fig. 2 C may suggest that the transition from closed to open state is voltage dependent. However, the linear I-V curve at divalent-free solution (Fig. 1 B) and the observation that divalent cations affect the mean open time (Fig. 3 D) negates this possibility.

The TRPL channel revealed bursting behavior (Fig. 4 B). This feature is a prominent characteristic of TRP channels in general (e.g., Shi et al., 2004). Bursting behavior of a channel is known to arise from fast transitions of the channel between a conducting (open state) and nonconducting closed or blocked states (see model in Fig. 4 A). The observation that two exponents are needed to best fit the open time histogram (Fig. 3 B) already suggested that two open states of long and short open times exist, though only a single conductance characterizes both (Fig. 2 A). To show that the two open states also exist in Ca^{2+}-free solutions where block is not expected, we constructed an open time histogram under these conditions, and two exponents were also needed to fit best the histogram (Fig. 4, C and E). At least three closed states of the channel must be assumed to account for the bursting behavior of the channel, in

which two distinct burst types were observed that differed in the mean open (Fig. 4 C) and closed times within the bursts (Fig. 4 D).

The model calculations tested the main issues of this work, namely the mechanism by which Ca^{2+} blocks the channel. To accommodate the model to the result showing that the mean open time is strongly reduced by Ca^{2+} (Fig. 3 D) we assumed in the model calculations that Ca^{2+} blocked the open channel (open channel block) and that depolarization relieved the channel from that block. Given that the TRPL channel has two open states, the results of Fig. 3 D suggested that only the long open state was susceptible to open channel block. Accordingly, a blocked state (B_2) was introduced into the model after the long open state (O_L). Since it was reasonable to assume that two open states with the same conductance share the same blocking properties, we added a blocked state (B_1) to the short open state (O_S) as well (see model insights below). Since Fig. 1 demonstrated that the divalent ion block occurs from both sides of the membrane (see also Hille, 1992) we set no limitation on the direction of divalent cation entry to the channel.

The result of Figs. 1 and 2 clearly showed that the TRPL channel exhibits voltage dependence in the presence of divalent cations. This result suggests that either entry of the channel or its exit from the blocked state is voltage dependent. To distinguish between these two possibilities we measured the mean closed time within the burst as a function of membrane voltage (Fig. 4 F). Fig. 4 F shows that the mean closed time becomes shorter at depolarizing voltage, indicating that k_b (the rate constant of exit from the blocked state) is voltage dependent. This conclusion was strongly supported by the model calculations as explained in model insights (supplemental text and Fig. S1). The model parameters that are listed in Table S3 were derived from direct experimental measurements (supplement) and account for all the above arguments.

Burst Duration and the Number of Channel Openings in a Burst Are Ca^{2+} and Voltage Dependent

A powerful way to explore the properties of the TRPL channel in general and the nature of the Ca^{2+} block in particular is to analyze the channel bursting behavior and its apparent voltage and Ca^{2+} dependence. Bursts are fast transitions of the channel between the open and the adjacent closed states. Thus, parameters that affect the burst, affect the open state. We therefore investigated burst properties with and without divalent cations at various membrane potentials. The design of these experiments was based on model predictions. Importantly, burst duration and the number of openings within the burst were independent of membrane potential in divalent free conditions when no block was expected, as predicted by the model (Fig. 5 A, right). In contrast, in the presence of divalent cations, an increase in membrane potential markedly increased the number of openings within the burst and consequently burst duration (Fig. 5 A, left). Furthermore, at negative membrane potential there were fewer events in the burst in the presence of divalent cations, and the burst duration became shorter relative to its duration in divalent-free condition, indicating that the blocked state terminates the burst. We consistently found that the criterion for burst definition (i.e., the time interval between channel openings within the burst) did not affect the conclusion that burst duration is strongly dependent on membrane potential in the presence of divalent cations (unpublished data). In the presence of divalent cations at positive membrane voltage, the number of events in the burst increased relative to divalent-free conditions (Fig. 5 B), indicating a stabilizing effect of the divalent cations on the burst. This observation indicates that the rate constant of TRPL-Ca^{2+} dissociation is voltage dependent (see Fig. S1).

Although the data of Fig. 5 were not employed to construct the model, channel activity and bursting behavior, calculated by a stochastic version of the model fit well the experimental data (not depicted). Furthermore, the model correctly predicted the dependence of channel opening frequency on membrane potential (solid line in Fig. 3 A). The differential version of the model also accurately predicted the outward rectifying I-V curve in the presence of divalent cations and the linear I-V relationship in their absence (Fig. 5 C).

Taken together, the excellent fit between the experimental data and model calculations strongly supports the important model prediction that TRPL–Ca^{2+} dissociation (and not association) is the voltage-dependent step that underlies the voltage dependence of the TRPL channel.

Divalent Cations Block Underlies the Voltage Dependence of the Native TRPL Channels

The results of Figs. 1–5 demonstrated that removal of Ca^{2+} block by positive voltage activated the TRPL channels by increasing the frequency of channel openings. Furthermore, the predictions of the kinetic model and TRPL channel bursting behavior indicated that voltage-dependent increase of the dissociation rate constant of Ca^{2+} from the blocked state underlies TRPL openings at positive membrane potential. Can open channel block by divalent cations, found in the expressed TRPL channels, also account for the voltage dependence of the native TRPL of the photoreceptor cells?

Before answering this question it is useful to outline several properties of the native versus the expressed TRPL channel and to address some of the problems involved in studying the effects of Ca^{2+} on the channels in the native photoreceptor cell. In the native system, the TRPL channel can be studied separately without the effects of the highly Ca^{2+}-permeable TRP channel, by

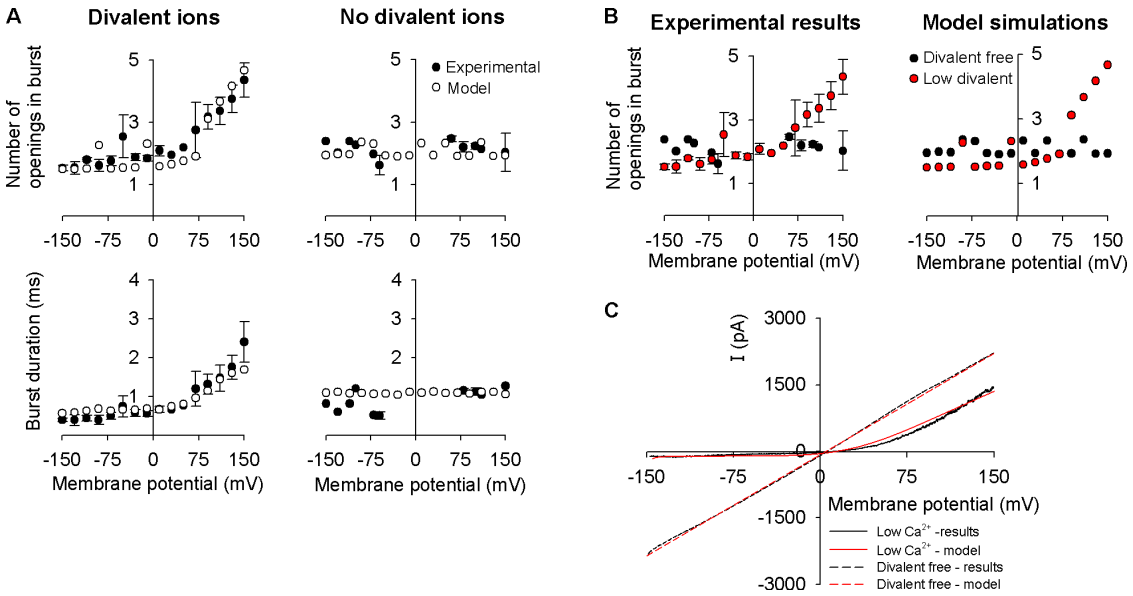

Figure 5. Burst duration and the number of channel openings in a burst are Ca^{2+} and voltage dependent; a comparison between experimental results and model predictions. (A) Voltage dependence of the bursting behavior obtained from single channel experiments with low divalent solution (solutions 2 and 5 in Tables I and II) or in divalent-free conditions (solutions 3 and 6 in Tables I and II). Two parameters were examined: burst duration and the number of events in the burst. ●, plots of the experimental results, ○, plots of the stochastic model simulation. Due to the stochastic nature of the model simulation, some variability in the calculated results is observed (n = 3–13). (B) The number of events in the burst with (red dot) and without (●) divalent cations (as in A) derived experimentally (left) and by model calculation (right). Note that at hyperpolarizing voltage, divalent cations shortened the burst duration, while at depolarizing voltage, the divalent ions stabilize the burst duration. Left, experimental results (n = 3–13). Right, stochastic model simulations. (C) Whole cell recorded I-V curves with and without divalent cations (solutions 2, 5 and 3, 6 in Tables I and II). The experimental results are compared with the model predictions as indicated.

using the *trp*^{P343} null mutant, which expresses only the TRPL channels (Scott et al., 1997). Although the characteristics of the native and expressed TRPL channel are similar, activation of the channel in the two systems is very different: Heterologously expressed TRPL channels in S2 cells are constitutively active (Hardie et al., 1997), while the native channels show their properties only during activation by light (Hardie and Minke, 1994b) or by metabolic stress (Hardie and Minke, 1994b; Agam et al., 2000; see below). Moreover, it is difficult to isolate the effects of Ca^{2+} on the native TRPL from its effects on the phospholipase Cβ (PLC), which activates TRPL, and its activity is strongly Ca^{2+} dependent (Berstein et al., 1992; Hardie et al., 2001). In wild-type fly, the major fraction of Ca^{2+} influx is via the Ca^{2+}-permeable TRP channel. The *trp* mutant, which expresses only TRPL channels, responds to sustained light transiently, revealing response inactivation due to an insufficient Ca^{2+} influx for normal PLC activity during prolonged lights (Hardie et al., 2001). This response inactivation is the hallmark of the *trp* mutant phenotype (Cook and Minke, 1999).

Long incubation of the photoreceptor cells in Ca^{2+}-free medium is required to obtain total removal of Ca^{2+} ions from the cytosol of these cells, due to their highly compartmentalized structure. However, prolonged Ca^{2+} deprivation abolishes light activation of the native channels (Cook and Minke, 1999; see also Agam et al., 2004). Therefore, we could examine the effect of Ca^{2+}-free solution for limited times only. We examined the effect of reducing Ca^{2+} levels on the I-V curve of the native TRPL channels either during shorts illuminations (1 s), or after metabolic exhaustion. Metabolic exhaustion induced TRPL channel openings in the dark after removal of ATP and GTP from the recording pipette. In both methods of channel activation, the magnitude of TRPL channel openings declined slowly (∼1 min) with time, and therefore, I-V curves were measured at maximal channel activity. When the extracellular solution contained 1.5 mM Ca^{2+}, virtually no inward current was observed at negative membrane potentials (Fig. 6 A, blue curves). In contrast, when no divalent cations were added to the extracellular solution (Low divalent), ∼1–2 nA inward current develops at −60 mV (Fig. 6 A, black). Further reduction of the Ca^{2+} level by adding EDTA (5 mM) to the intracellular and extracellular solutions resulted in >5 nA inward currents at −60 mV (Fig. 6 A, red curves). Importantly, the I-V curves measured after metabolic stress (Fig. 6 A) or light activation (Fig. 6 B) revealed similar dependence on Ca^{2+} concentrations, indicating that Ca^{2+} blocks the TRPL channel independent of the method of TRPL activation.

The large increase of the current in divalent-free conditions might arise from an unspecific leak current.

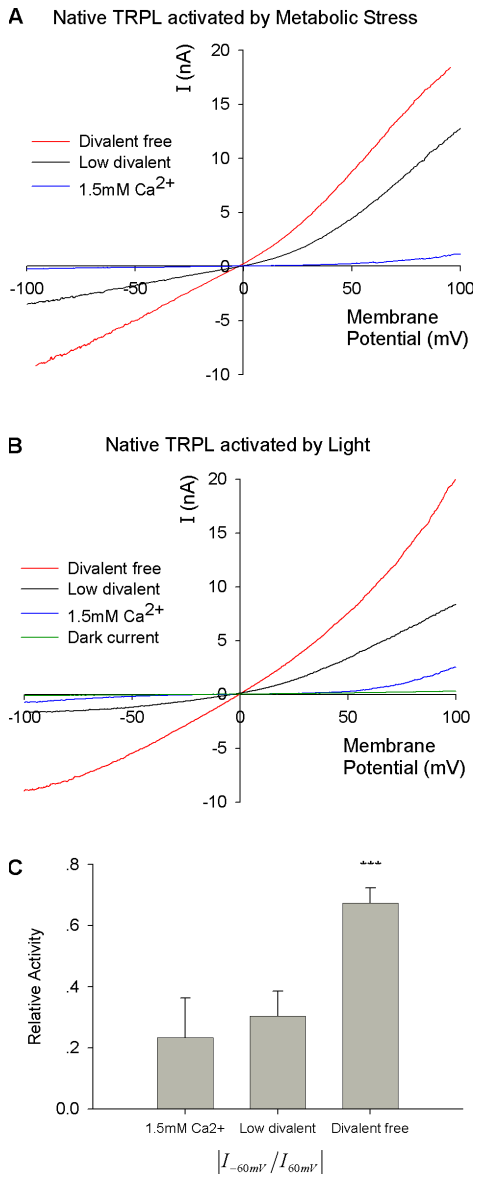

Figure 6. Open channel block by Ca^{+2} underlies the voltage dependence of the native TRPL channel. (A) I-V curves obtained using voltage ramps from −150 to 150 mV in 1 s (voltage ramps from 150 to −150 mV gave the same result) after channel activation by metabolic stress (see Materials and methods and text). Whole cell patch clamp recordings from the *Drosophila* isolated ommatidia of the trp^{P343} mutant at various Ca^{+2} concentration are shown (solutions 1, 4; 2, 5; and 3, 6 in Tables I and II). Although at maximal current some distortion of the I-V curve is expected, this distortion does not affect the conclusion that the I-V curve became nearly linear in divalent-free solution. (B) I-V curves obtained as in A during channel activation by light (orange OG 590, −logI = 0) at the same Ca^{2+} concentration as in A (solutions 1, 7; 2, 8; and 3, 9 in Tables I and II). (C) A quantitative analysis of the Ca^{2+}-induced block. The ratio of the current at −60 (I_{60}) and 60 mV (I_{60}) is presented. $P < 0.001$ (***); there is no significant difference between the left and middle columns ($n = 3–5$).

This possibility was ruled out by the following observations. First, after the cessation of the light stimulus in divalent-free conditions, the dramatic increase of both inward and outward currents during light was strongly suppressed, returning to the original small leak current in the dark (Fig. 6 B, green). Second, channel activation by metabolic stress is characterized by a transient increase in conductance (Hardie and Minke, 1994b). In divalent-free conditions after a nearly linear I-V curve was observed, the activated channels closed spontaneously and the current was reduced to a relatively small leak current (unpublished data). Together, these observations indicate that the near linearization of the I-V curve at divalent-free conditions is not the result of an increase in nonspecific leakage through the plasma membrane but a specific effect on the TRPL channels.

To quantitate the Ca^{2+}-dependent block of the inward current relative to the magnitude of the outward current, we calculated the ratio between the inward and outward currents at −60 and 60 mV membrane voltages, respectively, at different Ca^{2+} concentrations (Fig. 6 C). The small insignificant difference between the calculated ratio at 1.5 mM Ca^{2+} and low divalent is consistent with the high affinity of Ca^{2+} to the TRPL channel (Fig. 1 C). Importantly, the calculated ratio at divalent-free conditions is about twofold larger than under low divalent conditions, reflecting the almost linearity of the I-V curve (Fig. 6 A, red). Together, the study of the native TRPL channels indicates that their voltage dependence is not an intrinsic property but arises from Ca^{2+} block (Fig. 6).

DISCUSSION

Open Channel Block by Ca^{2+} Underlies the Voltage Dependence of *Drosophila* TRPL Channel

In the present study, the mechanism underlying the voltage dependence of the TRPL channel was investigated for the first time. The detailed analyses of single channel and whole cell currents indicated that the voltage dependence of the TRPL channel is not an intrinsic property but arises from open channel block by Ca^{2+}. The ability to robustly activate these channels at physiologically relevant negative membrane potentials by reducing Ca^{2+} levels was manifested by the appearance of a large inward current in the expressed and native TRPL channels. Previous reports showed only outward rectification of the TRPL channels (Chyb et al., 1999). However, Figs. 1 and 6 show that both the expressed and native TRPL channels revealed a pronounced conductance also at negative membrane potential in Ca^{2+} free conditions, which can be blocked by the presence of Ca^{2+} on both sides of the plasma membrane. This observation fits well with notion of voltage-dependent block by a permeable charged blocking agent that permeates the channel from both outside and inside the channel, while only depolarization can relieve this block (Hille, 1992; see also Seifert et al., 1999). Enhanced channel

openings at positive membrane potential of TRPL in the presence of divalent cations is fully consistent with the notion that Ca^{2+} open channel block underlies the outward rectification of these channels, because depolarization removes Ca^{2+} channel block. Similarly, channel openings at negative membrane potential in divalent-free conditions, when this block is reduced, support the above notion. The voltage-dependent Ca^{2+} block of the native TRPL channel (Fig. 6) is reminiscent of a very similar property of cyclic nucleotide-gated (CNG) channels, which was studied in great detail by Kaupp and colleagues (Seifert et al., 1999). This voltage-dependent blockage of the open channel is characteristic of positively charged, permeable channel blocker, where blockage efficacy increases when the membrane voltage is made less positive because access of Ca^{2+} to the blocking site in the channel lumen is facilitated (Seifert et al., 1999). The close similarity of the Ca^{2+} open channel block phenomenon between the TRPL channel and the thoroughly investigated CNG channels strongly supports the notion that the Ca^{2+} blocks the native TRPL channel by an open channel block mechanism.

Although the TRPL channel is a calmodulin (CaM) binding protein (Phillips et al., 1992; Scott et al., 1997), the blocking effect of Ca^{2+} on the channel most likely did not involve CaM because the blocking effect of Ca^{2+} was also found after application of Mg^{2+} and Ba^{2+}. This conclusion is supported by the findings of Flockerzi and colleagues who found that TRPL channel block by Ca^{2+} was not affected by calmidazolium, a known blocker of CaM and suggested that Ca^{2+} blocks the TRPL channel directly (Zimmer et al., 2000).

The difference in the mechanism underlying the voltage dependence of TRPC channels (i.e., TRPL) and the intrinsic voltage dependence of TRPV and TRPM channels (i.e., TRPV1 and TRPM8; Owsianik et al., 2005) may arise from the difference in the amino acid sequence at the pore region between the TRPC and TRPV&TRPM channels, which allows open channel block by Ca^{2+} in TRPL channels but not in TRPV channels (Owsianik et al., 2005). Taken together, the gating mechanism of the TRPL channel does not involve activation by voltage changes as suggested for TRPV and TRPM channels.

Physiological Implications of TRPL Channel Block by Ca^{2+}

The photoreceptor cell has two functional light-activated channels, TRP and TRPL. The TRP channels have a small (~4 pS) conductance (Hardie and Minke, 1994b), while the TRPL channels have much larger conductance of 110 pS (Fig. 2). The TRPL channels contribute ~40% to the total light-induced current in dark-adapted flies in response to dim or medium intensity lights (Bahner et al., 2002). At medium light intensities, the LIC is a sum of the current flow through both the TRP and TRPL channels (Reuss et al., 1997; Bahner et al., 2002). In contrast, during intense light, the LIC of WT flies is very similar to that of the *trpl* mutant (Niemeyer et al., 1996; Leung et al., 2000), indicating that the TRPL channels are inactive. This observation is readily explained by the higher Ca^{2+} affinity of the TRPL channels relative to the TRP channels (Hardie and Minke, 1994a; Reuss et al., 1997). (The lower Ca^{2+} affinity of the TRP relative to the TRPL channel is clearly reflected in I-V curves measured at nominal external Ca^{2+} [~10 μM external Ca^{2+}] in the relevant mutants. While the I-V curve of the *trp* mutant shows strong outward rectification and minimal inward current at nominal external Ca^{2+}, the *trpl* mutant [or WT flies] shows a strong inward and outward rectification at the same external Ca^{2+} concentration [Hardie and Minke, 1994a; Reuss et al., 1997].) Since the TRPL channel has large single channel conductance, it greatly contributes to the noise of the LIC (Reuss et al., 1997). It is therefore expected, according to an open channel block mechanism, that at intense light, when all TRPL channels are blocked, the noise level will be reduced. In contrast, at medium light intensities, when a large fraction of the TRPL channels is still available for light activation, the noise level will be higher. Indeed, the study of Hardie and colleagues (Reuss et al., 1997) shows that the noise level of the LIC induced by medium intensity light is significantly larger in WT than in the *trpl* mutant (with no TRPL channels). Taken together, the signal to noise ratio of the light response is improved during intense light by Ca^{2+} open channel block of the TRPL channel.

It is interesting to note that divalent open channel block that largely reduces the single channel conductance is a property of CNG channels of vertebrate photoreceptors, indicating that divalent open channel block is a general strategy of increasing the signal to noise ratio of photoreceptor cells in the animal kingdom (Gray and Attwell, 1985).

We thank Drs. Nathan Dascal, Bernard Attali, Ariela Gordon-Shaag, and Shahar Frechter for stimulating discussions and critical reading of the manuscript.

This research was supported by grants from the National Institutes of Health (EY 03529), The Israel Science Foundation, The Minerva Foundation, the US-Israel Binational Science Foundation, The German Israel Foundation, and the Israel-Korea Cooperation Program.

Lawrence G. Palmer served as editor.

Submitted: 31 August 2006
Accepted: 7 December 2006

REFERENCES

Agam, K., M. von-Campenhausen, S. Levy, H.C. Ben-Ami, B. Cook, K. Kirschfeld, and B. Minke. 2000. Metabolic stress reversibly activates the *Drosophila* light-sensitive channels TRP and TRPL in vivo. *J. Neurosci.* 20:5748–5755.

Agam, K., S. Frechter, and B. Minke. 2004. Activation of the *Drosophila* TRP and TRPL channels requires both Ca^{2+} and protein dephosphorylation. *Cell Calcium.* 35:87–105.

Bahner, M., S. Frechter, N. Da Silva, B. Minke, R. Paulsen, and A. Huber. 2002. Light-regulated subcellular translocation of *Drosophila* TRPL channels induces long-term adaptation and modifies the light-induced current. *Neuron.* 34:83–93.

Berstein, G., J.L. Blank, D.Y. Jhon, J.H. Exton, S.G. Rhee, and E.M. Ross. 1992. Phospholipase C-β1 is a GTPase-activating protein for Gq/11, its physiologic regulator. *Cell.* 70:411–418.

Chyb, S., P. Raghu, and R.C. Hardie. 1999. Polyunsaturated fatty acids activate the *Drosophila* light-sensitive channels TRP and TRPL. *Nature.* 397:255–259.

Clapham, D.E. 2003. TRP channels as cellular sensors. *Nature.* 426:517–524.

Clapham, D.E., D. Julius, C. Montell, and G. Schultz. 2005. International union of pharmacology. XLIX. Nomenclature and structure-function relationships of transient receptor potential channels. *Pharmacol. Rev.* 57:427–450.

Colquhoun, D., and A.G. Hawkes. 1995. The principles of the stochastic interpretation of ion-channel mechanisms. *In* Single-Channel Recording. B. Sakmann and E. Neher, editors. Plenum Press, New York. 397–482.

Colquhoun, D., and F.J. Sigworth. 1995. Fitting and statistical analysis of single channel recordings. *In* Single-Channel Recording. E. Neher and B. Sakmann, editors. Plenum Press, New York. 483–587.

Cook, B., and B. Minke. 1999. TRP and calcium stores in *Drosophila* phototransduction. *Cell Calcium.* 25:161–171.

Gillespie, D.T. 1977. Exact stochastic simulation of coupled chemical reactions. *J. Phys. Chem.* 81:2340–2361.

Gray, P., and D. Attwell. 1985. Kinetics of light-sensitive channels in vertebrate photoreceptors. *Proc. R. Soc. Lond. B. Biol. Sci.* 223:379–388.

Hambrecht, J., S. Zimmer, V. Flockerzi, and A. Cavalie. 2000. Single-channel currents through transient-receptor-potential-like (TRPL) channels. *Pflugers Arch.* 440:418–426.

Hardie, R.C. 1991. Whole-cell recordings of the light induced current in dissociated *Drosophila* photoreceptors: evidence for feedback by calcium permeating the light-sensitive channels. *Proc. R. Soc. Lond. B. Biol. Sci.* 245:203–210.

Hardie, R.C., and B. Minke. 1994a. Calcium-dependent inactivation of light-sensitive channels in *Drosophila* photoreceptors. *J. Gen. Physiol.* 103:409–427.

Hardie, R.C., and B. Minke. 1994b. Spontaneous activation of light-sensitive channels in *Drosophila* photoreceptors. *J. Gen. Physiol.* 103:389–407.

Hardie, R.C., and P. Raghu. 2001. Visual transduction in *Drosophila*. *Nature.* 413:186–193.

Hardie, R.C., H. Reuss, S.J. Lansdell, and N.S. Millar. 1997. Functional equivalence of native light-sensitive channels in the *Drosophila trp*^{301} mutant and TRPL cation channels expressed in a stably transfected *Drosophila* cell line. *Cell Calcium.* 21:431–440.

Hardie, R.C., P. Raghu, S. Moore, M. Juusola, R.A. Baines, and S.T. Sweeney. 2001. Calcium influx via TRP channels is required to maintain PIP_2 levels in *Drosophila* photoreceptors. *Neuron.* 30:149–159.

Hille, B. 1992. Ionic Channels of Excitable Membranes. Second edition. Sinauer Associates, Inc., Sunderland, MA. 607 pp.

Kunze, D.L., W.G. Sinkins, L. Vaca, and W.P. Schilling. 1997. Properties of single *Drosophila* Trpl channels expressed in Sf9 insect cells. *Am. J. Physiol.* 272:C27–C34.

Leung, H.T., C. Geng, and W.L. Pak. 2000. Phenotypes of *trpl* mutants and interactions between the transient receptor potential (TRP) and TRP-like channels in *Drosophila*. *J. Neurosci.* 20:6797–6803.

Minke, B., and B. Cook. 2002. TRP channel proteins and signal transduction. *Physiol. Rev.* 82:429–472.

Minke, B., and M. Parnas. 2006. Insights on *trp* channels from in vivo studies in *Drosophila*. *Annu. Rev. Physiol.* 68:649–684.

Minke, B., C. Wu, and W.L. Pak. 1975. Induction of photoreceptor voltage noise in the dark in *Drosophila* mutant. *Nature.* 258:84–87.

Montell, C. 1999. Visual transduction in *Drosophila*. *Annu. Rev. Cell Dev. Biol.* 15:231–268.

Montell, C. 2005. The TRP superfamily of cation channels. *Sci. STKE.* 2005:re3.

Niemeyer, B.A., E. Suzuki, K. Scott, K. Jalink, and C.S. Zuker. 1996. The *Drosophila* light-activated conductance is composed of the two channels TRP and TRPL. *Cell.* 85:651–659.

Nilius, B., and F. Mahieu. 2006. A road map for TR(I)Ps. *Mol. Cell.* 22:297–307.

Nilius, B., K. Talavera, G. Owsianik, J. Prenen, G. Droogmans, and T. Voets. 2005. Gating of TRP channels: a voltage connection? *J. Physiol.* 567:35–44.

Obukhov, A.G., C. Harteneck, A. Zobel, R. Harhammer, F. Kalkbrenner, D. Leopoldt, A. Luckhoff, B. Nurnberg, and G. Schultz. 1996. Direct activation of *trpl* cation channels by Gα11 subunits. *EMBO J.* 15:5833–5838.

Owsianik, G., K. Talavera, T. Voets, and B. Nilius. 2005. Permeation and selectivity of TRP channels. *Annu. Rev. Physiol.* 68:685–717.

Pedersen, S.F., G. Owsianik, and B. Nilius. 2005. TRP channels: an overview. *Cell Calcium.* 38:233–252.

Peretz, A., E. Suss-Toby, A. Rom-Glas, A. Arnon, R. Payne, and B. Minke. 1994. The light response of *Drosophila* photoreceptors is accompanied by an increase in cellular calcium: effects of specific mutations. *Neuron.* 12:1257–1267.

Phillips, A.M., A. Bull, and L.E. Kelly. 1992. Identification of a *Drosophila* gene encoding a calmodulin-binding protein with homology to the *trp* phototransduction gene. *Neuron.* 8:631–642.

Ranganathan, R., G.L. Harris, C.F. Stevens, and C.S. Zuker. 1991. A *Drosophila* mutant defective in extracellular calcium-dependent photoreceptor deactivation and rapid desensitization. *Nature.* 354:230–232.

Ranganathan, R., D.M. Malicki, and C.S. Zuker. 1995. Signal transduction in *Drosophila* photoreceptors. *Annu. Rev. Neurosci.* 18:283–317.

Reuss, H., M.H. Mojet, S. Chyb, and R.C. Hardie. 1997. In vivo analysis of the *Drosophila* light-sensitive channels, TRP and TRPL. *Neuron.* 19:1249–1259.

Scott, K., and C. Zuker. 1998. TRP, TRPL and trouble in photoreceptor cells. *Curr. Opin. Neurobiol.* 8:383–388.

Scott, K., Y. Sun, K. Beckingham, and C.S. Zuker. 1997. Calmodulin regulation of *Drosophila* light-activated channels and receptor function mediates termination of the light response in vivo. *Cell.* 91:375–383.

Seifert, R., E. Eismann, J. Ludwig, A. Baumann, and U.B. Kaupp. 1999. Molecular determinants of a Ca^{2+}-binding site in the pore of cyclic nucleotide-gated channels: S5/S6 segments control affinity of intrapore glutamates. *EMBO J.* 18:119–130.

Shi, J., E. Mori, Y. Mori, M. Mori, J. Li, Y. Ito, and R. Inoue. 2004. Multiple regulation by calcium of murine homologues of transient receptor potential proteins TRPC6 and TRPC7 expressed in HEK293 cells. *J. Physiol.* 561:415–432.

Voets, T., G. Droogmans, U. Wissenbach, A. Janssens, V. Flockerzi, and B. Nilius. 2004. The principle of temperature-dependent gating in cold- and heat-sensitive TRP channels. *Nature.* 430: 748–754.

Voets, T., K. Talavera, G. Owsianik, and B. Nilius. 2005. Sensing with TRP channels. *Nat. Chem. Biol.* 1:85–92.

Zimmer, S., C. Trost, U. Wissenbach, S. Philipp, M. Freichel, V. Flockerzi, and A. Cavalie. 2000. Modulation of recombinant transient-receptor-potential-like (TRPL) channels by cytosolic Ca^{2+}. *Pflugers Arch.* 440:409–417.